Int J Clin Exp Med 2019;12(1):337-346
www.ijcem.com /ISSN:1940-5901/IJCEM0080174

Original Article

Reconstruction of rabbit degenerated intervertebral discs using *SOX9* gene-modified bone marrow mesenchymal stem cells

Chongtao Zhu[1*], Ting Li[2,3*], Yongqing Xu[4], Qiang Guo[2,3], Xiaowen Qu[1]

[1]Laser Medical Center, [2]Deparment of Gastroenterology, The First People's Hospital of Yunnan Province, The Affiliated Hospital of Kunming University of Science and Technology, Kunming, Yunnan, China; [3]Faculty of Environmental Science and Engineering, Kunming University of Science and Technology, Kunming, Yunnan, China; [4]Orthopedic Center, Kunming General Hospital of Chengdu Military Command, Kunming, Yunnan, China. [*]Co-first authors.

Received May 23, 2018; Accepted August 3, 2018; Epub January 15, 2019; Published January 30, 2019

Abstract: Aims: Both the *SOX9* gene and bone marrow mesenchymal stem cells (BMSCs) have been applied for regeneration of degenerated intervertebral discs (IVDs) in animal models. However, whether the combined application of the *SOX9* gene and BMSCs improves the regeneration of IVDs has yet to be investigated. Materials and methods: In this study, recombinant adenovirus Ad-SOX9-GFP and Ad-GFP control were prepared and used to transfect BMSCs that were labeled with the red CM-DiI tracer. After establishing the IVD degeneration (IDD) rabbit model by aspirating the nucleus pulposus in L2-3, L3-4, and L4-5, a composite alginate hydrogel containing 2.5×10^7 recombinant BMSCs/ml was injected into these intervertebral spaces. During the 4th, 24th, and 48th weeks, the experimental animals were subjected to histological and morphological observation, spine X-ray imaging, MRI imaging, and IVD height index (DHI) calculation. Results: H&E staining showed that the BMSCs grew well and were evenly distributed in the IVD tissues. During the 48th week, immunohistochemical staining showed that there was more type II collagen expression in the IVD tissue of the experimental group than in the control group. Imaging showed that both the DHI values and the MRI T2 signals in the experimental group were significantly higher than those in the controls. Conclusion: BMSCs expressing the *SOX9* gene can significantly delay reduction of disc height and to some extent reverse degeneration of intervertebral discs in the rabbit IDD model, possibly through induction of BMSC differentiation into cartilage. These results suggest potential clinical applications of this novel strategy for treating IDD.

Keywords: *SOX9* gene, bone marrow mesenchymal stem cells, intervertebral disc degeneration, regeneration, type II collagen

Introduction

In clinical practice, it is generally believed that intervertebral disc degeneration (IDD) initiates a series of mechanical disorders of the spine and back pain. Current methods of treating disc herniation can be broadly divided into non-surgical and surgical therapies. Traditional spinal fusion surgery is considered the gold standard [1-3]. Evidence shows that after fusion, limitation of mid-body flexibility, changes in spine dynamics, and accelerated degeneration of adjacent segments occur, and these effects may lead to lumbar instability and the occurrence and recurrence of spinal stenosis [4, 5]. This observation has drawn attention to non-fusion technologies, including anterior-approach artificial disc replacement and posterior-approach non-fusion spine surgery [6]. Although non-fusion technologies do not share many of the drawbacks of spinal fusion surgery, none of these surgical treatments can alleviate all clinical symptoms. The IDD process cannot be reversed, and it is not possible to fundamentally reshape the anatomical structures and physiological functions of the intervertebral disc (IVD) [7]. Progress in studies of the pathological process and molecular mechanisms of IDD have suggested that biological methods of IDD intervention may make it possible to cure this disease.

One important pathological change associated with IDD is the loss of cartilage in the joint [8,

9]. Promoting chondrocyte activity and the generation of cartilage in the degenerated joint is a key to treating IDD. The *SOX9* gene belongs to the *SOX* gene family, and it is an important transcription factor for the synthesis of type II collagen and cartilage [10]. The *SOX9* gene is involved in regulating specific activation of the gene for type II collagen (*Col2al*) in chondrocytes, and *Col2al* is crucial for cartilage-specific cell differentiation [11]. Thus, the *SOX9* gene is also called the housekeeping gene of the chondrocyte phenotype, and its function in promoting the regeneration of degenerated IVDs has attracted a great deal of interest [12].

BMSCs are pluripotent cells, and this property makes them ideal seed cells [13, 14]. *In vitro* and *in vivo* studies have confirmed that BMSCs can differentiate into chondrocytes, osteoblasts, adipocytes, liver stem cells, muscle cells, heart cells, and other types of cells [15, 16]. For treatment of bone and cartilage defects, BMSC transplantation is a convenient and effective approach and has been investigated in several animal models [17, 18]. However, whether the SOX9 gene and BMSCs have synergistic effects in treating IDD remains to be elucidated.

To this end, in the present study, recombinant adenoviruses expressing SOX9 were prepared and used to transfect BMSCs. Then, a composite alginate hydrogel containing these recombinant BMSCs was injected into degenerated IVDs in a rabbit IDD model. The contribution of the recombinant BMSCs to the production of the nucleus pulposus (NP) extracellular matrix and the therapeutic efficacy of this approach for IDD were examined to provide experimental data for further potential preclinical trials.

Materials and methods

Reagents and instruments

An alginate hydrogel (Curapharm Inc., U.S.), premium fetal bovine serum (Gibco, U.S.), cell dissociation buffer (a mixture containing a final concentration of 0.25% trypsin and 0.02% EDTA), phosphate-buffered saline (PBS), Percell lymphocyte separation medium (Shanghai Plus Bio-Sci & Tech Co., Ltd., China), a pentobarbital sodium injection solution (Shanghai New Asia Pharmaceutical Co., Ltd., China), a 0.1% benzalkonium bromide solution, medical compound iodine solution (Sichuan Mingxing Pharmaceutical Co., Ltd., China), an IX71 inverted fluorescence microscope (Olympus, Japan), and a C-5050ZOOM digital camera (Olympus, Japan) were used in this study.

The CM-DiI red tracer (Sigma, U.S.), cell dissociation buffer (a mixture containing a final concentration of 0.25% trypsin and 0.02% EDTA), phosphate-buffered saline (PBS), Percell lymphocyte separation medium (Shanghai Plus Bio-Sci & Tech Co., Ltd., China), a pentobarbital sodium injection solution (Shanghai New Asia Pharmaceutical Co., Ltd., China), a 0.1% benzalkonium bromide solution, medical compound iodine solution (Sichuan Mingxing Pharmaceutical Co., Ltd., China), alginate hydrogels (Curapharm Inc., U.S.), premium fetal bovine serum (Gibco, U.S.), an IX71 inverted fluorescence microscope (Olympus, Japan), and a C-5050ZOOM digital camera (Olympus, Japan) were used in this study.

Recombinant virus

The Ad-SOX9-GFP recombinant adenovirus and the control Ad-GFP were provided by Dr. Youan Shang at the Southwest Hospital of the Third Military Medical University in Chongqing, China. The virus was purified and concentrated to 1×10^{10}/L [21].

Separation of primary BMSCs, gene transfection, and staining using the red fluorescent dye CM-DiI

Bilateral iliac crest bone marrow samples were collected from healthy 3-month-old New Zealand rabbits and subjected to density gradient centrifugation and adherence-based isolation. After two weeks of culture, a monolayer of passaged cells had formed. Rabbit BMSCs were cultured in 24-well culture plates until the fusion rate reached 80%, and three wells were randomly selected for cell counting. Based on a multiplicity of infection (MOI) value of 50, Ad-SOX9-GFP and control Ad-GFP were added. With PBS, the final volume was set at 100 μl. After 1 hour of transfection, each well was supplemented with 0.4 ml of 5% Dulbecco's modified Eagle's medium (DMEM), and the cells were cultured with 5% CO_2 at 37°C for 48 hours. A total of 24 rabbits with IDD were randomly divided into three groups of 8 each. Then, 1×10^6/L of the transgenic BMSC suspension

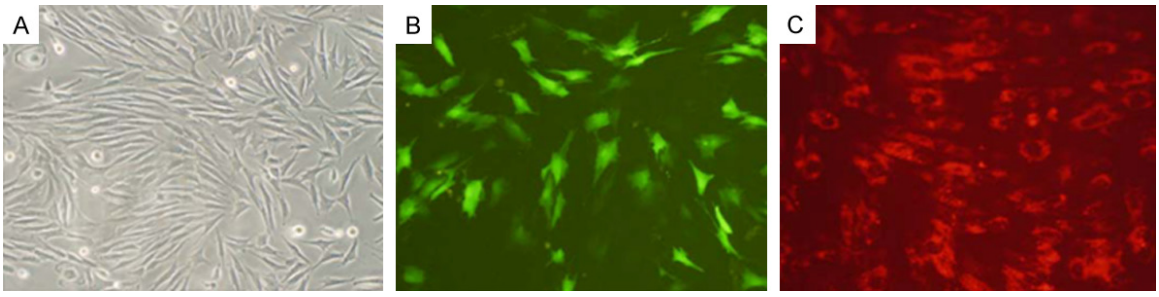

Figure 1. Primary BMSC culture (400×). Primary BMSCs were isolated from rabbit bone marrow and transfected with Ad-SOX9-GFP, followed by CellTracker™ CM-DiI staining. Morphology (A) and green (B, GFP) and red (C, CM-DiI) fluorescence were observed under an optical microscope or fluorescence microscope.

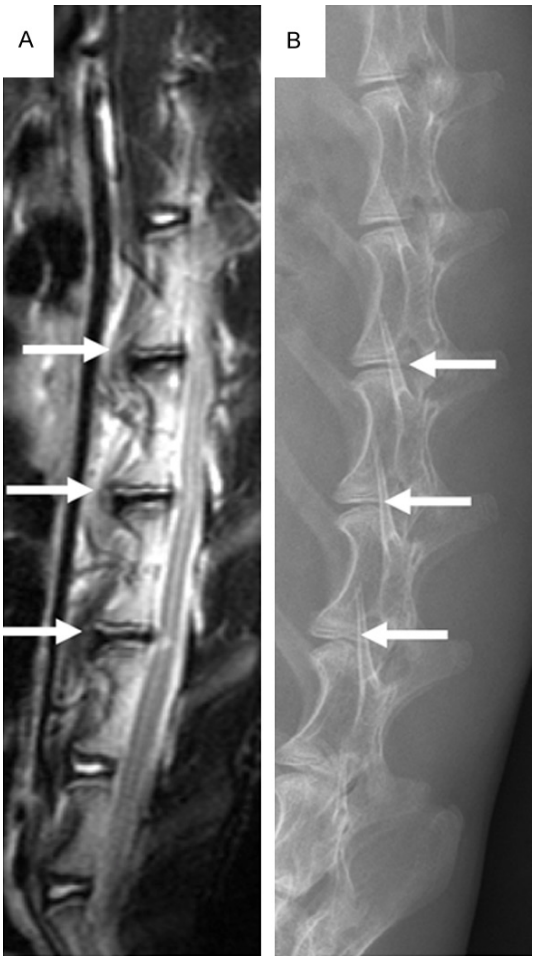

Figure 2. Imaging of the rabbit model 3 weeks after NP aspiration. MRI (A) and X-ray (B) exams after 3 weeks of NP aspiration. The white arrows indicate the L2/3, L3/4, and L4/5 IVD spaces.

was mixed with 2% alginate hydrogel (Curapharm Inc., U.S.). Using a microsyringe, 20 μl of this mixture was injected into the IVD spaces at L2/3, L3/4, and L4/5 in the experimental group. In the control group, 20 μl of alginate hydrogel at the same concentration was injected into the IVD spaces.

At 25°C, trypsin at a mass concentration of 2.5 g/L was used to digest cells in the logarithmic growth phase. The cells were then washed twice with PBS and centrifuged for 5 minutes. After the supernatant was carefully aspirated, 2 ml of serum-free DMEM was added, and the cells were then added to medium containing 4 mg/L CellTracker™ CM-DiI (Invitrogen China Limited, Beijing, China), mixed evenly and then placed in a 37°C incubator for 10 minutes, followed by centrifugation for 10 minutes. DMEM containing serum was used to wash the cells twice and to make a cell suspension. An appropriate amount of the cell suspension was examined under a fluorescence microscope to assess staining, the fluorescence intensity of the labeled epidermal cells and cell viability.

Establishment of a rabbit IDD model using nuclear aspiration

Healthy New Zealand white rabbits were subjected to intravenous 3% pentobarbital anesthesia. A longitudinal posterolateral incision was made in the abdomen, and via the extraperitoneal approach, the front lateral side of the vertebral body was reached (the transverse process was destroyed if necessary) to expose the L2/3, L3/4, and L4/5 IVD spaces. A 21G syringe needle was used to penetrate the IVD space at a depth of 5 mm. This process was performed a total of 5 times to damage the nucleus. A 5 ml syringe was used to aspirate the NP tissue. The wound was then sutured layer by layer, and measures were taken to prevent infection. L2/3, L3/4, and L4/5 IDD ani-

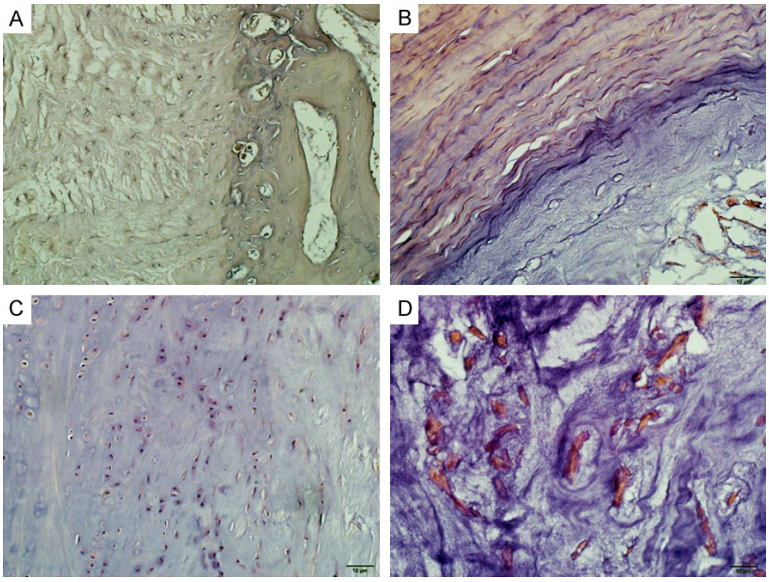

Figure 3. H&E staining of reconstructed IVDs. H&E staining was conducted for the nucleus of the normal rabbit IVD (A), the IDD model (B), and IDD rabbits transplanted with BMSCs modified by Ad-SOX9-GFP at 4 weeks (C) and 24 weeks (D).

mal models were established surgically [23, 24]. After three weeks, MRI examination was performed to assess changes in intervertebral height and T2 signaling.

H&E staining

Samples were collected during week 48 after surgery, and the labeled streptavidin biotin (LSAB) method was used for staining. The sample was first embedded in paraffin and then subjected to serial sectioning at 4 μm before dewaxing and hydration. Endogenous peroxidase was eliminated, antigens were retrieved, and the sections were blocked overnight at 4°C. Streptavidin-peroxidase (SP) solution was added, and sections were allowed to incubate for 40 minutes at 37°C. After diaminobenzidine (DAB) incubation, re-staining with hematoxylin, and dehydration, the sections were cleared and mounted with a neutral gum.

MRI and X-ray examination

The IDD models were established using the aspiration method. The 24 New Zealand rabbits were anesthetized using 3% sodium pentobarbital for MRI and X-ray examination. MRI T2 signaling and DHI were the main indicators examined. The T2 signals of the L2/3, L3/4, and L4/5 IVD spaces in the experimental and control groups were measured during weeks 24 and 48 after surgery. The DHI ratio (DHI%) was determined as follows: the heights of the front and rear edges of the IVD and the heights of the front and rear edges of the upper vertebral body were measured and used to calculate the DHI, and the DHI of the experimental group was then normalized to that of the control group (i.e., DHI (experimental group) %=DHI (experimental group)/DHI (control group)) [25, 26].

Statistical analysis

SPSS 13.0 software was used for statistical analysis of T2 values and DHI values. The data are expressed as the mean ± standard deviation (x ± s, n=8). T-tests were used for intergroup comparisons. $P<0.05$ was considered statistically significant.

Results

Transfection and labeling of BMSCs

After 12 hours of culturing primary BMSCs, most of the cells adhered to the bottom of the well, and most of the cells merged on days 9-10 (**Figure 1A**). The passaged cells showed vigorous growth, rapid proliferation, notable nuclei, and clear nucleoli. There were no significant changes in cell morphology before the 6th generation. BMSCs of the second generation were harvested and transfected with recombinant Ad-SOX9-GFP (target gene) and Ad-GFP (control) with a high transfection efficiency, as indicated by the intense fluorescence of GFP under a fluorescence microscope (**Figure 1B**). After staining with CellTracker™ CM-DiI, red fluorescence was observed in the Ad-SOX9-GFP-transfected BMSCs (**Figure 1C**). The two labeling techniques were combined to determine the survival time of the BMSCs and the time of the target gene effect.

Establishment of the IDD model

In degenerative IVDs, the nucleus was aspirated thoroughly (**Figure 2A**). The T2-weighted MRI signal of the degenerative discs decreased

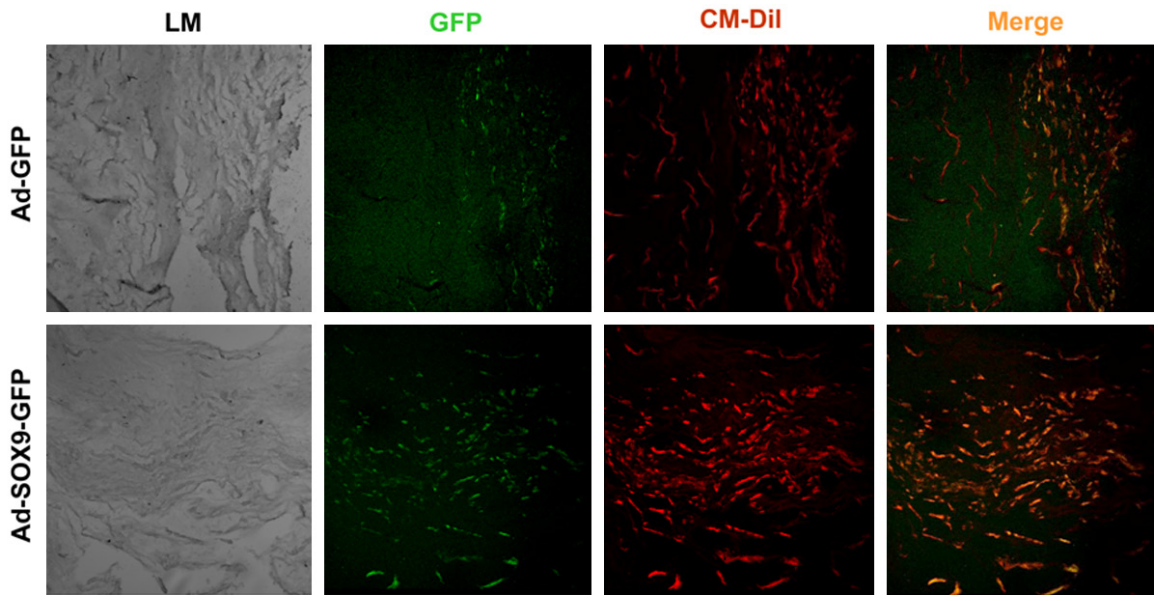

Figure 4. Nucleus after the transplantation of Ad-SOX9-GFP/BMSCs. Forty-eight weeks after transplantation with Ad-SOX9-GFP or the Ad-GFP control, the experimental IVDs were harvested and observed under a light microscope (LM) or fluorescence microscope for GFP (green) and CM-DiI (red) fluorescence in the transfected BMSCs in the IVDs.

substantially (**Figure 2A**). The disc height decreased, and vertebral hyperostosis was observed, possibly due to the reduced volume of the nuclear tissue, the decreased hydrostatic pressure, the instability of the upper and lower vertebral bodies and the stress redistribution in the nucleus caused by reduced water content (**Figure 2A**). An anteroposterior X-ray scan at levels L2-5 showed clear bird-peck-like protrusions formed by bone hyperplasia at the front edges of the corresponding upper and lower vertebral bodies (**Figure 2B**).

Morphology of the IVDs reconstructed by Ad-SOX9-GFP/BMSCs

Light microscopy showed that, with H&E staining in the control group, the central nucleus was round and raised toward the cartilage endplate. In the peripheral area, fibrous tissue was arranged in an annular shape and stained pink, and the boundary between the central nucleus and the fibrous ring was clear (**Figure 3A**). However, in the IDD group, nuclear tissues were incomplete, and the boundary between the nucleus and the peripheral fibrous ring was unclear. Some of the peripheral annular fibrous tissues entered the central nucleus, and there were fewer cells in the central zone (**Figure 3B**). In the IDD group, 4 weeks after BMSC transplantation, the central nucleus was relatively complete, and the boundary between the nucleus and the surrounding fibrous ring was clear. The nucleus and cytoplasm were clearly stained and showed clear boundaries. In the central nucleus, the cells aggregated into lumps, and cell clones were formed by 3-5 cells (**Figure 3C**). At 24 weeks after treatment, NP-like tissues were roughly generated (**Figure 3D**).

Immunofluorescence of the IVDs reconstructed by Ad-SOX9-GFP/BMSCs

The IVD nucleus tissues of the IDD rabbit model after transplantation with Ad-SOX9-GFP/BMSCs or the Ad-GFP control were examined by detecting double-labeled fluorescence under the fluorescence microscope 48 weeks after transplantation. As shown in **Figure 4**, stronger GFP green fluorescence and CM-DiI cell tracker red fluorescence were observed in Ad-SOX9-GFP/BMSC-transplanted nuclei than in the Ad-GFP control group. Furthermore, the GFP and CM-DiI fluorescence almost completely merged, indicating the successful transplantation of the recombinant BMSCs in the IDD model.

X-ray examination of the IVDs reconstructed by Ad-SOX9-GFP/BMSCs

The methods of calculating DHI and comparing groups that were described by Lu et al. were

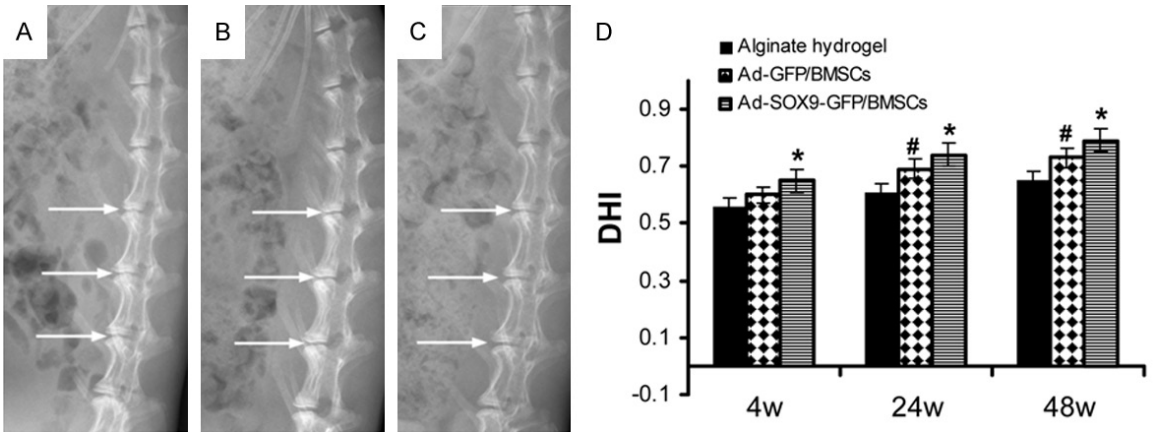

Figure 5. X-ray examination. X-ray exams were conducted 48 weeks after transplantation of the composite alginate hydrogel (A), the Ad-GFP/BMSCs (B) or the Ad-SOX9-GFP/BMSCs (C). The white arrows indicate the L2/3, L3/4, and L4/5 IVD spaces. The average IVD height in each group during weeks 4, 24, and 48 after the transplantations was measured (D). *, $P<0.05$ *vs* all other groups; #, $P<0.05$ *vs* the alginate hydrogel group.

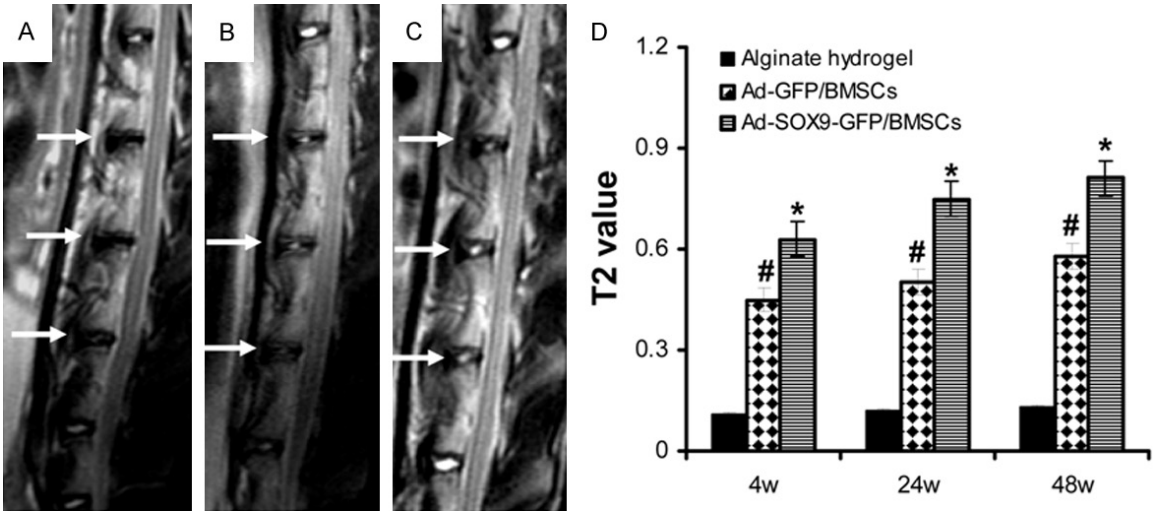

Figure 6. MRI examination. MRI exams were conducted 48 weeks after transplantation of the composite alginate hydrogel (A), the Ad-GFP/BMSCs (B) or the Ad-SOX9-GFP/BMSCs (C). The white arrows indicate the L2/3, L3/4, and L4/5 IVD spaces. The average T2 value during weeks 4, 24, and 48 after transplantation in each group was measured (D). *, $P<0.01$ *vs* all other groups; #, $P<0.01$ *vs* the alginate hydrogel group.

used in this study [26]. X-ray examinations revealed that the DHI value of the Ad-SOX9-GFP/BMSC-transplanted group was higher than those of the IDD model group and the Ad-GFP/BMSC control group (**Figure 5A-C**). Bone hyperplasia was visible at the front edges of the upper and lower vertebral bodies, and the changes in disc height were more substantial in the IDD model than in the Ad-SOX9-GFP/BMSC or Ad-GFP/BMSC groups (**Figure 5A-C**). A comparison of the average IVD height between the three groups showed that the negative control group, i.e., the composite alginate hydrogel group, had the narrowest IVDs. However, administration of Ad-SOX9-GFP/BMSCs and even Ad-GFP/BMSCs significantly rescued this damage, although the former treatment demonstrated stronger effects than the latter treatment (**Figure 5D**).

MRI examination of the IVDs reconstructed by Ad-SOX9-GFP/BMSCs

To further explore the effects of SOX9/BMSCs on the recovery of the damaged IVDs, an MRI examination was conducted. The results indi-

cated that 48 weeks after transplantation, the IVDs at L2-5 in the three groups exhibited lower signals than the T2-weighted signal of the normal IVD nucleus (**Figure 6A-C**). However, the T2 signal of the NP tissue in the Ad-SOX9-GFP/BMSC group was significantly higher than those in the alginate hydrogel control and Ad-GFP/BMSC groups. Furthermore, the Ad-GFP/BMSCs also showed a marked enhancement of the T2-weighted signal compared to the alginate hydrogel (**Figure 6A-C**).

In the Ad-GFP/BMSC group, the T2-weighted signals of the NP tissues in L2-L3, L3-L4, and L4-L5 were very weak immediately after transplantation, but over time, the signals recovered significantly. The T2-weighted signals in the Ad-SOX9-GFP/BMSC group, in which SOX9-modified BMSCs were transplanted into IVDs, were significantly higher at all time points than those of the other groups (**Figure 6D**), suggesting an active role of SOX9-modified BMSCs in delaying the progress of IDD. In addition, in comparison with the DHI values during weeks 4, 24, and 48 after transplantation (**Figure 5**), the MRI examination was more sensitive (**Figure 6**) and thus might be one of the best approaches for assessing the degeneration and restoration of IVDs.

Discussion

CM-DiI can be embedded in cell membranes to mark the whole cell. In recent years, it has been increasingly used as a tracer in studies of cell transplantation. CM-DiI is simple to use, stains quickly, has a slow fluorescence decay, and labels very efficiently. In the present study, enhanced green fluorescent protein (EGFP) and CM-DiI were used to label BMSCs in order to explore effective labeling methods for tracing the outcome of seed cells *in vivo*. The two labeling techniques were combined to determine the survival time of BMSCs and the time of the target gene effect.

Gene therapy for IDD involves introducing different target genes via gene transfection into IVD cells in order to increase the number of disc cells, maintain the IVD cell phenotype, and enhance the ability of disc cells to secrete extracellular matrix, thereby slowing or even reversing the pathological disc degeneration process. One study by Nishida et al. found that TGF-β can increase polysaccharide secretion in rabbit IVDs, and *in vitro* experiments have confirmed that human IVD tissues can respond to TGF-β, with significantly increased rates of prostaglandin and type II collagen production [27]. Paul et al. transfected SOX9 genes into human IVD cells using adenovirus [28] and found that SOX9 promoted the synthesis of type II collagen. Saka et al. performed BMSC transplantation 2 weeks after the establishment of a rabbit NP degeneration model [29]. An atelocollagen scaffold was transplanted before transplantation of the donor cells. Preliminary results indicated that after the transplantation of MSCs, the degeneration of IVDs was delayed, and the IVD function was improved.

In the 1980s, Owen first proposed the concept of marrow stromal stem cells (MSCs) [30]. It has been demonstrated that MSCs can be stimulated *in vitro* to differentiate into bone, cartilage, fat, nerve, and muscle cells and other types of mesenchymal cells. MSCs have a wide range of sources, possess high biological activity, and thus have unparalleled advantages over IVD cells. After many generations of amplification, MSCs maintain their differentiation potential [31]. However, it is precisely because of the high differentiation potential of MSCs that they undergo so little division *in vivo*. Whether exogenous target genes can be successfully transfected into MSCs and expressed is an important concern.

Adenoviruses are a non-integrating virus. After injection into cells, adenoviruses do not insert their own genetic material into the cell chromosome. Under conditions that allow non-integrating additional genes to exist, their DNA is contained in the cell nucleus. Adenoviruses are easily acquired, high-titer viruses and have a high infection rate for both dividing and non-dividing cells, although expression of the transferred gene may decrease over time [21]. In the present study, the SOX9 gene served as the target gene, and adenovirus was used as the carrier to transfect the target gene into BMSCs, which were then mixed with an alginate hydrogel for injection into the rabbit IDD model. The purpose of this approach was to evaluate the efficacy of IDD treatment using genetically modified stem cells. Imaging showed that one month after the surgery, the T2-weighted MRI signals and DHI values in the experimental

group started to become higher than the values observed in the control group. These differences were significant 6 months and 12 months after surgery. Histological results showed that during week 48 after surgery, the intensity of green fluorescent protein in the IVDs of the control group was reduced, and there were fewer cells than before. This change might occur because some of the exogenous MSCs did not adapt to the internal environment of the IVD and exhibited reduced function (reduced protein expression) or because some of the cells had died, and the decrease in the number of cells led to a corresponding reduction in expression of the corresponding effector protein, type II collagen. However, during week 48 after surgery, the intensity of green fluorescent protein in the IVDs of the experimental group, the density and intensity of the fluorescence of the BMSCs, and the expressed effector protein level still remained relatively high. This outcome might have occurred because after a period of time, the MSCs had adapted to the internal environment of the IVD, and the target gene SOX9 played a substantial role. Specifically, this approach accelerated differentiation of BMSCs modified by SOX9 into cartilage and caused type II collagen to be overexpressed. This change increased the water content in the NP and played a key role in reversing or delaying IDD.

The significance of the present study is as follows. The selected seed cells, BMSCs, served two therapeutic purposes. They were not only the carriers of the target gene, which caused them to continuously secrete exogenous SOX9 protein and promote disc tissue repair, but they also directly induced differentiation *in vivo* to promote the synthesis of the IVD cell matrix, further facilitating IVD tissue repair. CM-DiI-labeled BMSCs combined with alginate hydrogel were transplanted into the degenerative IVD, and pathological sections showed that, after transplantation, the BMSCs survived in the degenerated IVD. The number of transplanted cells gradually decreased for a period of time and then held steady, and the cells started to differentiate into chondrocytes. These microscopic observations provide a scientific basis for follow-up studies. In conclusion, the advantages of MSC transplantation and gene therapy were combined, and a simple, highly efficient, and practical new method of treating IDD, the use of genetically modified stem cells and tissue-engineered NP, was evaluated. The preliminary results were as expected. In the near future, the use of gene therapy in combination with tissue engineering based on cells and scaffolds may prove even more promising [32, 33].

Acknowledgements

This work was financially supported by the Basic Research Program of Yunnan Province (No. 2009CD123) and Key Research Program of China (No. YS2018YFB040045).

Disclosure of conflict of interest

None.

Address correspondence to: Qiang Guo, Deparment of Gastroenterology, The First People's Hospital of Yunnan Province, The Affiliated Hospital of Kunming University of Science and Technology, Kunming, Yunnan, China; Faculty of Environmental Science and Engineering, Kunming University of Science and Technology, Kunming, Yunnan, China. E-mail: 1502899051@qq.com; Xiaowen Qu, Laser Medical Center, The First People's Hospital of Yunnan Province, The Affiliated Hospital of Kunming University of Science and Technology, 157 Jinbi Road, Kunming, Yunnan, China. Tel: +86 13888579646; Fax: +86 871-63611582; E-mail: quyishengtougao@126.com

References

[1] Quraishi NA, Konig M, Booker SJ, Shafafy M, Boszczyk BM, Grevitt MP, Mehdian H, Webb JK. Access related complications in anterior lumbar surgery performed by spinal surgeons. Eur Spine J 2013; 22 Suppl: S16-20.

[2] Pelton MA, Phillips FM, Singh K. A comparison of perioperative costs and outcomes in patients with and without workers' compensation claims treated with minimally invasive or open transforaminal lumbar interbody fusion. Spine 2012; 37: 1914-1919.

[3] Fengbin Y, Deyu C, Xinwei W, Yu C, Jinhao M, Xinyuan L, Xiaowei L. Trauma-induced spinal cord injury in cervical spondylotic myelopathy with or without lower cervical instability. J Clin Neurosci 2013; 20: 419-422.

[4] Komura S, Miyamoto K, Hosoe H, Iinuma N, Shimizu K. Lower incidence of adjacent segment degeneration after anterior cervical fusion found with those fusing C5-6 and C6-7 than those leaving C5-6 or C6-7 as an adjacent level. J Spinal Disord Tech 2012; 25: 23-29.

[5] Holinka J, Krepler P, Matzner M, Grohs JG. Stabilising effect of dynamic interspinous spacers in degenerative low-grade lumbar instability. Int Orthop 2011; 35: 395-400.
[6] Ilharreborde B, Shaw MN, Berglund LJ, Zhao KD, Gay RE, An KN. Biomechanical evaluation of posterior lumbar dynamic stabilization: an in vitro comparison between universal clamp and wallis systems. Eur Spine J 2011; 20: 289-296.
[7] Reyes-Sanchez A, Zarate-Kalfopulos B, Ramirez-Mora I, Rosales-Olivarez LM, Alpizar-Aguirre A, Sanchez-Bringas G. Posterior dynamic stabilization of the lumbar spine with the accuflex rod system as a stand-alone device: experience in 20 patients with 2-year follow-up. Eur Spine J 2010; 19: 2164-2170.
[8] Bisschop A, van Royen BJ, Mullender MG, Paul CP, Kingma I, Jiya TU, van der Veen AJ, van Dieen JH. Which factors prognosticate spinal instability following lumbar laminectomy? Eur Spine J 2012; 21: 2640-2648.
[9] Massey CJ, van Donkelaar CC, Vresilovic E, Zavaliangos A, Marcolongo M. Effects of aging and degeneration on the human intervertebral disc during the diurnal cycle: a finite element study. J Orthop Res 2012; 30: 122-128.
[10] Davies SR, Chang LW, Patra D, Xing X, Posey K, Hecht J, Stormo GD, Sandell LJ. Computational identification and functional validation of regulatory motifs in cartilage-expressed genes. Genome Res 2007; 17: 1438-1447.
[11] Ushijima T, Okazaki K, Tsushima H, Iwamoto Y. CCAAT/Enhancer binding protein beta regulates the repression of type II collagen expression during the differentiation from proliferative to hypertrophic chondrocytes. J Biol Chem 2014; 289: 2852-63.
[12] Wan R, Hu J, Zhou Q, Wang J, Liu P, Wei Y. Application of co-expressed genes to articular cartilage: new hope for the treatment of osteoarthritis (review). Mol Med Rep 2012; 6: 16-18.
[13] Ren J, Stroncek DF, Zhao Y, Jin P, Castiello L, Civini S, Wang H, Feng J, Tran K, Kuznetsov SA, Robey PG, Sabatino M. Intra-subject variability in human bone marrow stromal cell (BMSC) replicative senescence: molecular changes associated with BMSC senescence. Stem Cell Res 2013; 11: 1060-1073.
[14] Wang Y, Mostafa NZ, Hsu CY, Rose L, Kucharki C, Yan J, Jiang H, Uludag H. Modification of human BMSC with nanoparticles of polymeric biomaterials and plasmid DNA for BMP-2 secretion. J Surg Res 2013; 183: 8-17.
[15] Retraction of "Co-culture of microtic chondrocyte with BMSC to generate tissue engineered cartilage". Tissue Eng Part A 2012; 18: 1530.
[16] Kachgal S, Carrion B, Janson IA, Putnam AJ. Bone marrow stromal cells stimulate an angiogenic program that requires endothelial MT1-MMP. J Cell Physiol 2012; 227: 3546-3555.
[17] Yagami K, Shirota T, Shintani S, Mayahara M, Nishizawa M, Yanagisawa S, Sammons R, Kuboki Y. Honeycomb form beta-tricalcium phosphate induces osteogenesis by geometrical property with BMSC. Biomed Mater Eng 2011; 21: 291-306.
[18] Zeis B, Becher B, Lamkemeyer T, Rolf S, Pirow R, Paul RJ. The process of hypoxic induction of Daphnia magna hemoglobin: subunit composition and functional properties. Comp Biochem Physiol B Biochem Mol Biol 2003; 134: 243-252.
[19] Acosta FL Jr, Lotz J, Ames CP. The potential role of mesenchymal stem cell therapy for intervertebral disc degeneration: a critical overview. Neurosurg Focus 2005; 19: E4.
[20] Kepler CK, Ponnappan RK, Tannoury CA, Risbud MV, Anderson DG. The molecular basis of intervertebral disc degeneration. Spine J 2013; 13: 318-330.
[21] Wiethoff CM, Middaugh CR. Barriers to nonviral gene delivery. J Pharm Sci 2003; 92: 203-217.
[22] Huang W, Carlsen B, Wulur I, Rudkin G, Ishida K, Wu B, Yamaguchi DT, Miller TA. BMP-2 exerts differential effects on differentiation of rabbit bone marrow stromal cells grown in two-dimensional and three-dimensional systems and is required for in vitro bone formation in a PLGA scaffold. Exp Cell Res 2004; 299: 325-334.
[23] Iwashina T, Mochida J, Sakai D, Yamamoto Y, Miyazaki T, Ando K, Hotta T. Feasibility of using a human nucleus pulposus cell line as a cell source in cell transplantation therapy for intervertebral disc degeneration. Spine 2006; 31: 1177-1186.
[24] Sakai D, Mochida J, Iwashina T, Watanabe T, Nakai T, Ando K, Hotta T. Differentiation of mesenchymal stem cells transplanted to a rabbit degenerative disc model: potential and limitations for stem cell therapy in disc regeneration. Spine 2005; 30: 2379-2387.
[25] Kim KS, Yoon ST, Li J, Park JS, Hutton WC. Disc degeneration in the rabbit: a biochemical and radiological comparison between four disc injury models. Spine (Phila Pa 1976) 2005; 30: 33-7.
[26] Lu DS, Shono Y, Oda I, Abumi K, Kaneda K. Effects of chondroitinase ABC and chymopapain on spinal motion segment biomechanics. An in vivo biomechanical, radiologic, and histologic canine study. Spine 1997; 22: 1828-1834; discussion 1834-1825.

[27] Misra S. Human gene therapy: a brief overview of the genetic revolution. J Assoc Physicians India 2013; 61: 127-133.
[28] Paul R, Haydon RC, Cheng H, Ishikawa A, Nenadovich N, Jiang W, Zhou L, Breyer B, Feng T, Gupta P, He TC, Phillips FM. Potential use of Sox9 gene therapy for intervertebral degenerative disc disease. Spine 2003; 28: 755-763.
[29] Sakai D, Mochida J, Yamamoto Y, Nomura T, Okuma M, Nishimura K, Nakai T, Ando K, Hotta T. Transplantation of mesenchymal stem cells embedded in atelocollagen gel to the intervertebral disc: a potential therapeutic model for disc degeneration. Biomaterials 2003; 24: 3531-3541.
[30] Owen M. Marrow stromal stem cells, Journal of cell science. Supplement 1988; 10: 63-76.
[31] Quintin A, Schizas C, Scaletta C, Jaccoud S, Applegate LA, Pioletti DP. Plasticity of fetal cartilaginous cells. Cell Transplant 2010; 19: 1349-1357.
[32] See EY, Toh SL, Goh JC. Effects of radial compression on a novel simulated intervertebral disc-like assembly using bone marrow-derived mesenchymal stem cell cell-sheets for annulus fibrosus regeneration. Spine 2011; 36: 1744-1751.
[33] O'Halloran DM, Pandit AS. Tissue-engineering approach to regenerating the intervertebral disc. Tissue Eng 2007; 13: 1927-1954.